Optimal F-domain stabilization technique for reduction of commensurate fractional-order SISO systems

MAHATA, S.; HERENCSÁR, N.; ALAGOZ, B. B.; YEROGLU, C.

Fractional Calculus and Applied Analysis
vol. 25

ISSN 1311-0454

DOI: http://dx.doi.org/10.1007/s13540-022-00014-6

Accepted manuscript

Fract. Calc. Appl. Anal. manuscript No. FCAA-D-21-00003
(will be inserted by the editor)

Optimal F-domain stabilization technique for reduction of commensurate fractional-order SISO systems

Shibendu Mahata[1] · **Norbert Herencsar**[2] ·
Baris Baykant Alagoz[3] ·
Celaleddin Yeroglu[3]

Received: 10 December 2021 / Revised: 24 February 2022 / Accepted: 27 February 2022

Abstract This paper presents a new approach for reduction of commensurate fractional-order single-input-single-output systems. The minimization in the frequency response error of the reduced order model (ROM) relative to the original system is carried out in the F-plane. A constrained optimization technique is introduced to satisfy the angle criteria for F-domain stability of the proposed ROM. Significant improvements in both the time- and frequency-responses over the recently published literature are illustrated using several numerical examples.

Keywords fractional-order system (primary) · commensurate system · F-domain · model order reduction · optimization · reduced order model · stability

Mathematics Subject Classification (2010) 26A33 (primary) 93C10 · 93C80 · 93E99

1 Introduction

Fractional calculus is a branch of mathematics which deals with the generalization of the differentiation and integration operations, see for example [5],

Shibendu Mahata[1]
Department of Electrical Engineering, Dr. B. C. Roy Engineering College, Durgapur, West Bengal, PO – 713206, India
E-mail: shibendu.mahata@bcrec.ac.in

Norbert Herencsar[2,*]
Department of Telecommunications, Faculty of Electrical Engineering and Communication, Brno University of Technology, Technicka 12, 616 00 Brno, Czechia
E-mail: herencsn@vut.cz * corresponding author

Baris Baykant Alagoz and Celaleddin Yeroglu[3]
Department of Computer Engineering, Faculty of Engineering, Inonu University, 44000 Malatya, Turkey
E-mail: baykant.alagoz@inonu.edu.tr; c.yeroglu@inonu.edu.tr

[28]. It has attracted attention of both pure mathematicians and applied scientists due to wide range of applications of fractional-order (FO) models in natural and social sciences, economics, control theory, etc., we may refer the readers to survey [20]. Various definitions of the FO differintegral operators are available as shortly outlined below; for details see e.g. [28].

(i) *Riemann-Liouville (R-L) definition*

Considered as an extension of the n-fold successive integration, the αth-order integration ($\alpha \geq 0$) is given by

$$ {}_aD_t^{-\alpha} f(t) := \frac{1}{\Gamma(\alpha)} \int_a^t (t-\tau)^{\alpha-1} f(\tau) d\tau, \ \alpha > 0, \tag{1.1} $$

where $f(t)$ is a function for which the integral in (1.1) exists, and $\Gamma(\cdot)$ denotes the Euler gamma function.

The R-L definition for the αth-order, where $n-1 < \alpha < n$, derivative of $f(t)$ is defined as

$$ {}_aD_t^{\alpha} f(t) := \frac{1}{\Gamma(n-\alpha)} \frac{d^n}{dt^n} \int_a^t (t-\tau)^{n-\alpha-1} f(\tau) d\tau. \tag{1.2} $$

The Laplace transform of (1.2) is

$$ L\left\{ {}_0D_t^{\alpha} f(t) \right\} = s^{\alpha} F(s) - \sum_{k=0}^{n-1} s^k D^{\alpha-k-1} f(0+), \tag{1.3} $$

where $L\{\cdot\}$ denotes the Laplace transform operator; $L\{f(t)\} = F(s)$; and s^{α} is called the FO Laplacian operator. We have to note that no physical interpretation exists of the initial conditions for the R-L definition, $D^{(\alpha-k-1)} f(0+)$, while the definition of the Caputo fractional derivative (see [28], §2.4.1 and (2.140)) includes the initial conditions as $f(0), f'(0), f''(0), ...$, that allow their utilization.

(ii) *Grünwald-Letnikov (G-L) definition*

The G-L definition is based on the generalization of the backward difference rule.

$$ {}_aD_t{}^{\alpha} f(t) := \lim_{h \to 0} \frac{1}{h^{\alpha}} \sum_{j=0}^{\left[\frac{t-a}{h}\right]} (-1)^j \binom{\alpha}{j} f(t-jh) \ , \tag{1.4} $$

where $[x]$ denotes the integer part of x, and $\binom{\alpha}{j} = \dfrac{\Gamma(\alpha+1)}{\Gamma(j+1)\Gamma(\alpha-j+1)}$ represents the binomial coefficients.

Under zero initial conditions, the Laplace transformation of (1.2) and (1.4) leads to

$$ L\{ {}_0D_t^{\alpha} f(t)\} = s^{\alpha} F(s). \tag{1.5} $$

A fractional-order transfer function (FOTF) can be represented as

$$H_{FO}(s) = \frac{a_M s^{M-1+\lambda_P} + a_{M-1} s^{M-2+\lambda_{P-1}} + ... + a_1 s^{\lambda_1} + a_0}{b_N s^{N-1+\lambda_Q} + b_{N-1} s^{N-2+\lambda_{Q-1}} + ... + b_1 s^{\lambda_1^{'}} + b_0}, \tag{1.6}$$

where $M, N \in Z^+$; $0<\lambda_P$, λ_Q, λ_{P-1}, λ_{Q-1}, ..., λ_1, $\lambda_1^{'} < 1$; a_i $(i = 0, 1, \ldots, M)$ and b_j $(j = 0, 1, \ldots, N)$ are the coefficients of the numerator and denominator polynomials of $H_{FO}(s)$. The integer-order transfer function (IOTF) is a particular case of $H_{FO}(s)$ when $\lambda_P = \lambda_Q = \lambda_{P-1} = \lambda_{Q-1} = ... = \lambda_1 = \lambda_1^{'} = 1$. The impedance characteristics of the FO Laplacian operator s^α can be practically realized using the fractance elements or emulated using commercial electronic components [15], [17]. Applications of FO system modeling and their superiority over the traditional (integer-order) ones are highlighted in various disciplines such as control engineering [34], image processing [41], filter theory [22], etc.

Model order reduction (MOR) deals with order diminution while preserving the essential characteristics (e.g., stability, transient behavior, magnitude, phase) of the higher-order system [3]. Reduction of large-scale IO systems based on rational approximants has been widely investigated for the past several decades. Seminal techniques in this regard are the truncated balanced realization [26], singular perturbation [19], etc. Compression of FO systems using IO models is reported in [16], [40].

A recent work demonstrated that MOR of IO systems using FOTF achieved improved accuracy compared to the IOTF-based reduced order models (ROM) [6]. The superior performance of the compressed FO model in capturing the dynamics of the large-scale system may be attributed to the additional flexibility yielded from the non-integer exponents of s in its transfer function. The global reduction (e.g., direct truncation) and local reduction (e.g., Pade approximation) techniques were employed for MOR of commensurate FO systems and the ROM was obtained as a commensurate FOTF [33]. Representation of FO controllers based on commensurable transfer functions was demonstrated in [14]. Reduction of FO system based on retention of dominant dynamics was reported in [32]. MOR was carried out on Krylov subspaces for linear FO systems in [11]. The Arnoldi algorithm matched a specific number of moments of the ROM with the original system [18]; the technique was extended to solve MOR problems for FO systems in [13]. The Arnoldi algorithm attains stable ROM when the original system is a stable one. The approximation error between the ROM and the original system can be minimized in the frequency-domain by the Lanczos algorithm [2]. Although the number of matched moments for the Lanczos algorithm is double than that of the Arnoldi method, however, stability is not assured for the ROM designed using the Lanczos process [9]. Stable MOR of FO system using the unsymmetric Lanczos algorithm was recently reported [10]. The integral square error (ISE), defined as $\int_0^\infty \left[y_{O,S}(t) - y_{R,S}(t)\right]^2 dt$, where $y_{O,S}(t)$ and $y_{R,S}(t)$ are the unit-step responses of the original and reduced systems, respectively, was used as the objective function for diminution of commensurate FO systems using the

big bang–big crunch optimization (BBCO) algorithm [12]. The mixed-method reduction scheme of [4] where the numerator and denominator polynomials of the IO-ROM were determined using BBCO algorithm and time moment matching method, respectively, was extended in [30] to yield the reduced commensurate FOTF. In [27], an extended continued fraction expansion (CFE) method was demonstrated for the MOR of commensurate FO systems.

This paper introduces an optimal F-domain-based approach for the MOR of linear time-invariant (LTI) commensurate FO single-input-single-output (SISO) systems. The primary contributions of this paper are the following:

1. The stability of the proposed ROM is guaranteed by incorporating the critical phase in the F-plane ($F = s^{\alpha}$, $0 < \alpha < 2$) as a design inequality constraint. The suggested approach to satisfy the stability of the compressed FO model is different from the stability technique reported in [37] where the V-plane ($V = s^{1/p}$, where $\alpha = k/p$, with k and p being positive integers) method was used to design the FO proportional-integral-derivative controller. The objective function in [37] was minimized with respect to the target minimum angle root position inside the stable region of the first Riemann sheet, while the alteration of model parameters was incorporated as bound constraints to define the interval uncertainty. Furthermore, it is worth emphasizing that the BBCO-based optimization method published in [12] is an unconstrained one, which may not always produce a stable ROM.
2. The proposed objective function is formulated based on the minimization of frequency-domain behavior of the FO system, whereas the time-domain (ISE) behavior was considered in [12]. Three design examples are considered to demonstrate the markedly superior frequency and time-domain response matching of the proposed ROMs as compared to those of the recent literature. While previous works have reported the frequency-domain-based design of FO controllers [8], this research may be the first attempt to carry out the optimal fitting between the frequency characteristics of the original (large-scale) model and the reduced-order approximant for the commensurate FO systems directly in F-plane.

In the rest of the paper, Section 2 presents the proposed technique. Simulation results demonstrating the ROM stability and performance comparisons with the recent literature are discussed in Section 3. Finally, the paper concludes in Section 4.

2 Proposed Technique

Consider the LTI, SISO, proper, and commensurate FO system defined by

$$H_O(s) = \frac{\sum_{i=0}^{M} b_i (s^\alpha)^i}{\sum_{j=0}^{N} a_j (s^\alpha)^j}, \tag{2.1}$$

where b_i $(i = 0, 1, \ldots, M)$ and a_j $(j = 0, 1, \ldots, N)$ are the coefficients of the numerator and denominator polynomials of $H_O(s)$; b_i, $a_j \in \Re$; $N > M$; and $0 < \alpha < 2$.

The ROM can be modeled as

$$H_R(s) = \frac{\sum_{i=0}^{m} d_i (s^\alpha)^i}{\sum_{j=0}^{n} c_j (s^\alpha)^j}, \tag{2.2}$$

where d_i $(i = 0, 1, \ldots, m)$ and c_j $(j = 0, 1, \ldots, n)$ are the coefficients of the numerator and denominator polynomials of $H_R(s)$; d_i, $c_j \in \Re$; $m < n$; $m < M$; and $n < N$. Stability studies for a mapping function of the form $F = s^\alpha$ [29] have demonstrated that:

1. For $\alpha \leq 1$ $(\alpha > 1)$ the unstable region in the F-plane is smaller (larger) than that of the s-plane. This implies that the stable F-domain region reduces as α is increased;
2. Intersections in the F-plane occur between the stable regions for $1 < \alpha < \frac{4}{3}$ or between the stable and unstable regions for $\frac{4}{3} < \alpha < 2$;
3. System exhibits oscillatory behavior for $\alpha = 2$ and becomes unstable for $\alpha > 2$; and
4. The stability region in the F-plane is attained if the absolute minimum phase angle of the roots $(|\theta_F|)$ is greater than the critical phase angle $\theta_{Cr} = 0.5\alpha\pi$, where θ_F and θ_{Cr} are expressed in radians (rad).

Substituting $F = s^\alpha$ in (2.1) and (2.2) leads to the F-domain transfer function representations of the original and reduced models, respectively, as given by

$$H_O(F) = \frac{\sum_{i=0}^{M} b_i F^i}{\sum_{j=0}^{N} a_j F^j}, \tag{2.3}$$

$$H_R(F) = \frac{\sum_{i=0}^{m} d_i F^i}{\sum_{j=0}^{n} c_j F^j}. \tag{2.4}$$

Integer-valued exponents of F for the numerator and denominator polynomials of $H_O(F)$ and $H_R(F)$ are possible due to the commensurate form of the FOTF. The $F = s^\alpha$ mapping function is applicable when dealing with fractional derivatives, which are always multiples of α. In contrast, the V-plane [1], [36], [37] (also known as the W-plane [29]) transformation is more pertinent when α can be expressed as any rational number.

Therefore, a stable ROM may be designed in the F-plane by formulating a constrained optimization problem with the objective function f, which minimizes the frequency-domain error relative to the original model subject to the F-domain stability condition.

$$f = \sum_{i=1}^{L} \left| |H_O(F,\omega_i)| - |H_R(F,\omega_i,X)| \right| + \left| \angle H_O(F,\omega_i) - \angle H_R(F,\omega_i,X) \right|, \tag{2.5}$$

$$\text{Subject to: } |\theta_F| > \theta_{Cr},$$

where $|\theta_F|$ represents the minimum absolute phase angle attained from the n number of roots of the characteristic equation for $H_R(F)$, i.e., $\sum_{j=0}^{n} c_j F^j = 0$; $F = s^\alpha$; ω is the frequency in radians per second (rad/sec); L represents the total number of sampled frequency points spaced in a logarithmic fashion in the range $[\omega_{\min}, \omega_{\max}]$ rad/sec; and the decision variables vector is given by $X = [d_m \ d_{m-1} \ \dots \ d_0 \ c_n \ c_{n-1} \ \dots \ c_0]$. The dimension (D) of the problem is $m + n + 2$. The frequency-domain representation of $F = s^\alpha$ is given by $(j\omega)^\alpha = \omega^\alpha \angle(\alpha\pi/2)$. The purpose of the optimization routine is to determine the value of X which satisfies the design constraint and also achieves the least fitting error in the F-domain between the proposed ROM and the original system. Finally, the optimal s-domain transfer function for the proposed ROM can be obtained by replacing F with s^α in (2.4), which results in (2.2).

3 Simulation Results and Discussions

Metaheuristic techniques have demonstrated promising performance in dealing with nonlinear and non-convex optimization problems, including reduced order modeling [16], [21]. Inspired by the intelligence sharing process or evolutionary phenomena of organisms in nature, these algorithms can also efficiently handle constrained optimization problems [25]. The proposed FO MOR design problem is solved using the constrained composite differential evolution (C^2oDE)

[38] and the feasibility rule with incorporation of objective function information (FROFI) [39] algorithms. For the sake of brevity, the detailed framework of C^{2}oDE and FROFI is not discussed here. Recent works have exemplified the effectiveness of C^{2}oDE in designing optimal and stable FO digital filters [23], [24]. In this work, the population size and termination criteria for both the algorithms are selected as 100 and 10000$\times D$ objective function evaluations, respectively. All the simulations are carried out in MATLAB, with L = 100, $\omega_{\min} = 10^{-2}$ rad/sec, and $\omega_{\max} = 10^5$ rad/sec. The performance of the proposed method is illustrated using three design examples taken from the recent literature. Time-domain performance indices such as the integral absolute error (IAE), ISE, integral time absolute error (ITAE), and integral time square error (ITSE) are considered to quantify the modeling performance [7]. Frequency-domain error metrics such as the maximum and mean values of absolute magnitude error (AME) and absolute phase error (APE), mean square error (MSE) about the magnitude and phase, and the H_∞ norm [31], are also used to evaluate the accuracy of the reduced models.

$$\|H\|_\infty = \|H_O(s) - H_R(s)\|_\infty = \max_{\omega>0} |H_O(j\omega) - H_R(j\omega)| \,. \tag{3.1}$$

3.1 Example 1

Consider the following all-pole commensurate original FO system.

$$H_O(s) = \frac{250}{s^{0.6} + 15.88s^{0.4} + 42.46s^{0.2} + 106.2}. \tag{3.2}$$

The BBCO-based ROM reported in [12] is given by

$$H_R(s) = \frac{-0.15s^{0.2} + 96.38}{6.25s^{0.4} + 16.162s^{0.2} + 41.05} \tag{3.3}$$

To provide a fair comparison with [12], the F-domain transfer function for the proposed technique is chosen as per (2.4) with $m = 1$ and $n = 2$. The lower bound (Lb) and upper bound (Ub) of the design variables are chosen as [–30 0 0 0 0] and [30 30 30 30 30], respectively. The optimal value of X based on the C^{2}oDE algorithm is obtained as [-0.6648 19.9933 1.3075 2.9166 8.5665] which results in the poles being located at -1.1153 ± 2.3039i in the F-plane. Hence, the phase angles of the roots are given by $\pm115.83°$. Since $|\theta_F| = 115.83°$ is larger than $\theta_{Cr} = 18°$, therefore, the proposed model is stable in the F-domain. The locations of the poles in the F-plane for the designed ROM are shown in Fig. 1, which illustrates that the poles lie in the stable region. Resubstituting $s^{0.2} = F$, the C^{2}oDE-based ROM in the s-domain is obtained as

$$H_R(s) = \frac{-0.6648s^{0.2} + 19.9933}{1.3075s^{0.4} + 2.9166s^{0.2} + 8.5665}. \tag{3.4}$$

The FROFI algorithm yields X = [-0.9984 29.9836 1.9623 4.3699 12.8499]; hence, the pole locations in the F-plane are -1.1135 ± 2.3040i. The F-domain

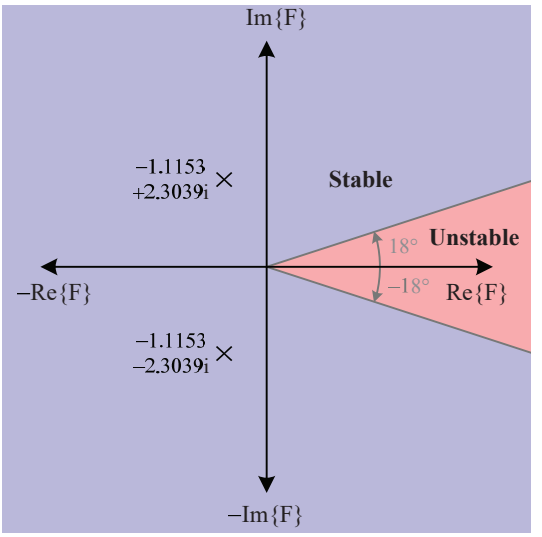

Fig. 1 Locations of poles in the F-plane for the proposed C^{2}oDE-based ROM in Example 1

stability condition is also satisfied for this design since $|\theta_F|\,(= 115.79°) > \theta_{Cr}(= 18°)$. The s-domain based compressed model yielded using FROFI is given by

$$H_R(s) = \frac{-0.9984s^{0.2} + 29.9836}{1.9623s^{0.4} + 4.3699s^{0.2} + 12.8499}. \tag{3.5}$$

It may be noted that although the values of X attained using C^{2}oDE and FROFI algorithms are different, the normalized values of the optimal design coefficients are nearly the same. For example, carrying out the normalization of X with respect to coefficient c_2 results in $X = [-0.5085\ 15.2912\ 1.0000\ 2.2307\ 6.5518]$ and $[-0.5088\ 15.2798\ 1.0000\ 2.2269\ 6.5484]$, respectively, for the C^{2}oDE and FROFI-based designs. This implies proximity in the locations of the zeros and poles in the the F-plane for both the optimal approximants. Hence, a close agreement may be expected in the performances of the ROMs designed using C^{2}oDE and FROFI.

Comparisons about the various frequency response performance metrics are presented in Table 1, which highlight the lower errors achieved by the designed models as compared to [12]. For instance, $\|H\|_\infty$ for the ROM designed using C^{2}oDE (0.00421) and FROFI (0.00440) is significantly lower than that of the BBCO method [12] (0.04970). The similarity in the performances of C^{2}oDE and FROFI-based ROMs can be also confirmed from the results presented in Table 1. Comparisons with [12] about the magnitude and phase responses, as shown in Fig. 2, demonstrate the superior accuracy of the proposed technique in approximating the characteristics of the original system. The error $e(j\omega) = |H_O(s) - H_R(s)|_{s=j\omega}$ for both the proposed designs is markedly

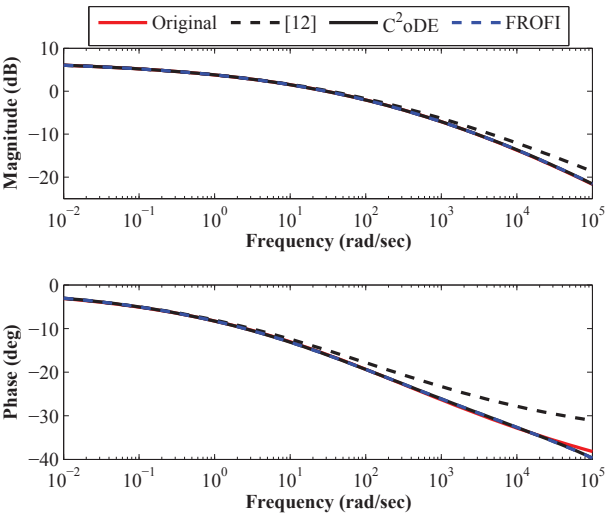

Fig. 2 Comparison of magnitude and phase responses of the proposed ROMs with the literature for Example 1

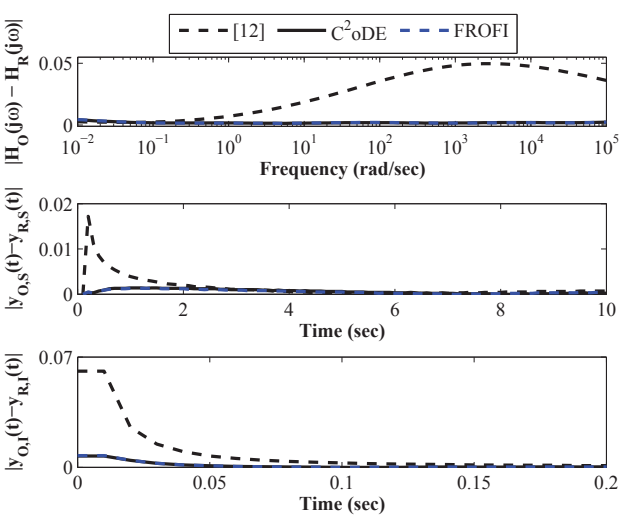

Fig. 3 Comparison of the proposed ROMs with the literature about the absolute error in frequency response (top), step response (middle), and impulse response (bottom) for Example 1

smaller compared to [12], as demonstrated in Fig. 3 (top). Note that similar response curves are achieved for the C^2oDE and FROFI-based designs.

Error metric	[12]	C^2oDE	FROFI
Max AME	0.0442	0.0033	0.0035
Mean AME	0.0214	0.0013	0.0013
Max APE (rad)	0.1242	0.0264	0.0267
Mean APE (rad)	0.0348	0.0027	0.0027
MSE for magnitude	7.46×10^{-4}	2.04×10^{-6}	2.08×10^{-6}
MSE for phase (rad^2)	0.0026	2.58×10^{-5}	2.64×10^{-5}
$\|H\|_\infty$	0.04970	0.00421	0.00440

Table 1 Comparisons with the literature about various frequency-domain performance indices for Example 1

Reference	IAE	ISE	ITAE	ITSE
[12]	0.01269	8.05×10^{-5}	0.0362	1.12×10^{-4}
C^2oDE	0.00560	5.46×10^{-6}	0.0210	1.64×10^{-5}
FROFI	0.00512	4.51×10^{-6}	0.0201	1.37×10^{-5}

Table 2 Comparisons with the literature about various time-domain performance indices for Example 1

The step and impulse responses of the FOTFs are determined using the FOMCON toolbox in MATLAB [35]. The absolute error curves for both these time responses of the C^2oDE and FROFI-based models are compared with the published literature [12] in Fig. 3 (middle and bottom). Note that $y_{O,I}(t)$ and $y_{R,I}(t)$ represent the impulse responses of the original system and the ROM, respectively. The proposed models achieve lower step response and impulse response errors in the time interval [0, 2] sec and [0, 0.14] sec, respectively, when compared to [12]. It may be observed that both the optimally designed proposed ROMs demonstrate similar time-domain behavior. Table 2 shows the performance comparisons of the C^2oDE and FROFI-based designs with [12], which confirm that the proposed approach achieves smaller IAE, ISE, ITAE, and ITSE. The ROM designed using FROFI attains marginally better accuracy than C^2oDE for all the time-domain performance indices. Although the objective function of the proposed method and [12] are based on minimization of errors in the frequency- and time-domain, respectively, however, the suggested technique can outperform the cited literature in both domains.

3.2 Example 2

Consider another original FO commensurate SISO system as given by

$$H_O(s) = \frac{s^4 + 9s^{3.2} + 31s^{2.4} + 58.01s^{1.6} + 60.01s^{0.8} + 16.03}{s^{4.8} + 6s^4 + 48s^{3.2} + 286s^{2.4} + 935s^{1.6} + 1580s^{0.8} + 888}. \quad (3.6)$$

The Arnoldi algorithm [13] and unsymmetric Lanczos algorithm [10] based ROMs are respectively reported as

$$H_R(s) = \frac{0.6459s^{2.4} + 1.2085s^{1.6} + 1.2501s^{0.8} + 0.3339}{s^{3.2} + 5.9584s^{2.4} + 19.4920s^{1.6} + 32.9168s^{0.8} + 18.5003}, \tag{3.7}$$

$$H_R(s) = \frac{1.0737s^{2.4} + 3.0549s^{1.6} + 6.5803s^{0.8} + 2.1319}{s^{3.2} + 4.3930s^{2.4} + 18.7373s^{1.6} + 132.4863s^{0.8} + 118.1308}. \tag{3.8}$$

Therefore, the proposed ROM in the F-domain can be considered as per (2.4) with $m = 3$ and $n = 4$. The objective function minimization is carried out by selecting Lb and Ub for all the design variables as 0 and 100, respectively. The optimal value of X is attained as [1.0298 2.4014 3.2091 0.9448 1.0000 0.0000 33.6919 74.6944 52.1202] for the C^{2}oDE-based reduced system. The locations of the poles for the designed approximant $H_R(F)$ are $\{1.0572\pm5.9688\text{i}, -1.0572\pm0.5484\text{i}\}$. Hence, the polar form representation of the poles of $H_R(F)$ is given as $\{6.0617\angle \pm 79.96°, 1.1910\angle \pm 152.58°\}$. Since $\theta_{Cr} = 72°$ is smaller than $|\theta_F| = 79.96°$, therefore, the stability of the designed ROM is confirmed. Fig. 4 justifies the stability of the C^{2}oDE-based design by highlighting the absence of poles in the unstable region of the F-plane. After retro-fitting from F-domain to s-domain, the transfer function of the C^{2}oDE-based model can be obtained as

$$H_R(s) = \frac{1.0298s^{2.4} + 2.4014s^{1.6} + 3.2091s^{0.8} + 0.9448}{1.0000s^{3.2} + 33.6919s^{1.6} + 74.6944s^{0.8} + 52.1202}. \tag{3.9}$$

The FROFI algorithm yielded X = [1.0564 2.2407 3.2275 1.0003 1.0001 0.0000 33.8247 69.9989 55.0322] for the same design problem. Therefore, the locations of the poles for the ROM are $\{1.0047\pm5.9444\text{i}, -1.0047\pm0.7103\text{i}\}$, i.e., $\{6.0287\angle \pm 80.40°, 1.2304\angle \pm 144.74°\}$, in the complex F-plane. The F-domain stability of the model is assured since $|\theta_F| = 80.40°$ exceeds the critical value $\theta_{Cr} = 72°$. The FROFI-based ROM transfer function in the s-domain is given by

$$H_R(s) = \frac{1.0564s^{2.4} + 2.2407s^{1.6} + 3.2275s^{0.8} + 1.0003}{1.0001s^{3.2} + 33.8247s^{1.6} + 69.9989s^{0.8} + 55.0322}. \tag{3.10}$$

Error metric	[10]	[13]	C^{2}oDE	FROFI
Max AME	0.3177	0.5236	0.0183	0.0163
Mean AME	0.0133	0.0264	7.52×10^{-4}	7.78×10^{-4}
Max APE (rad)	1.0054	1.3023	0.0296	0.0372
Mean APE (rad)	0.0566	0.1511	0.0058	0.0068
MSE for magnitude	0.0023	0.0071	4.59×10^{-6}	4.42×10^{-6}
MSE for phase (rad^2)	0.0222	0.1080	9.91×10^{-5}	1.49×10^{-4}
$\|H\|_\infty$	0.45140	0.53650	0.01836	0.01890

Table 3 Comparisons with the literature about various frequency-domain performance indices for Example 2

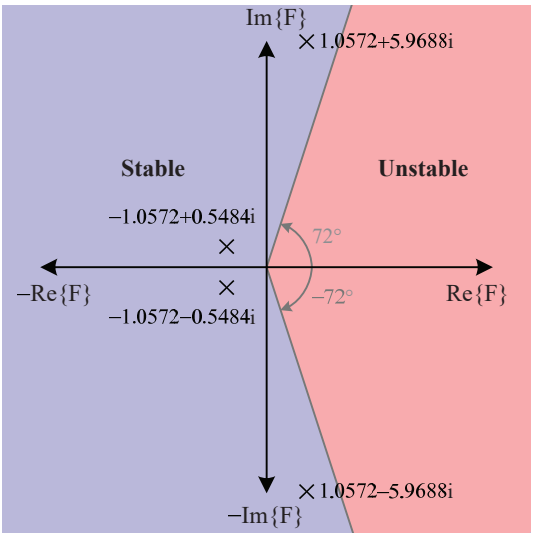

Fig. 4 Locations of poles in the F-plane for the proposed C^{2}oDE-based ROM in Example 2

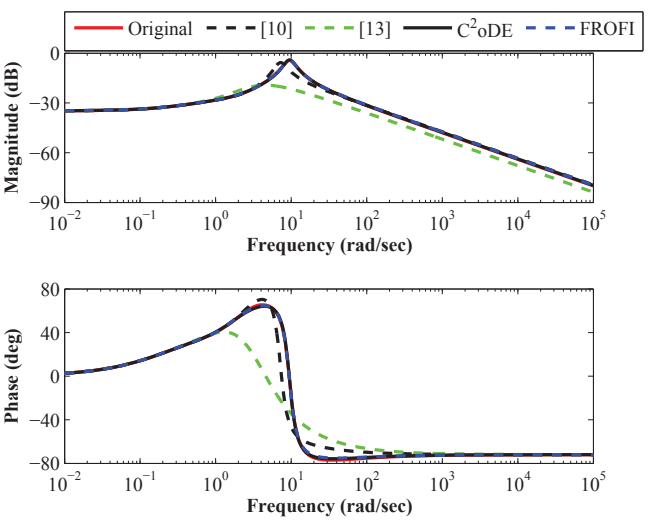

Fig. 5 Comparisons of magnitude and phase responses of the proposed ROMs with the literature for Example 2

As shown in Fig. 5, the magnitude and phase responses of both the optimally designed ROMs exhibit better proximity with the original systems' behavior as compared to the models reported in [10], [13]. The responses of the C^{2}oDE and FROFI-optimized models nearly superimpose on the theoretical (large-scale system) characteristics. Comparisons about $e(j\omega)$ with the published designs, as presented in Fig. 6, justify the lower error of the pro-

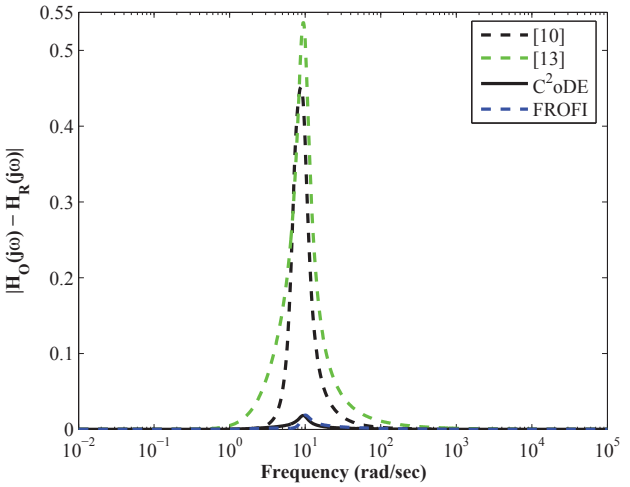

Fig. 6 Comparisons of absolute error in frequency response of the proposed ROMs with the literature for Example 2

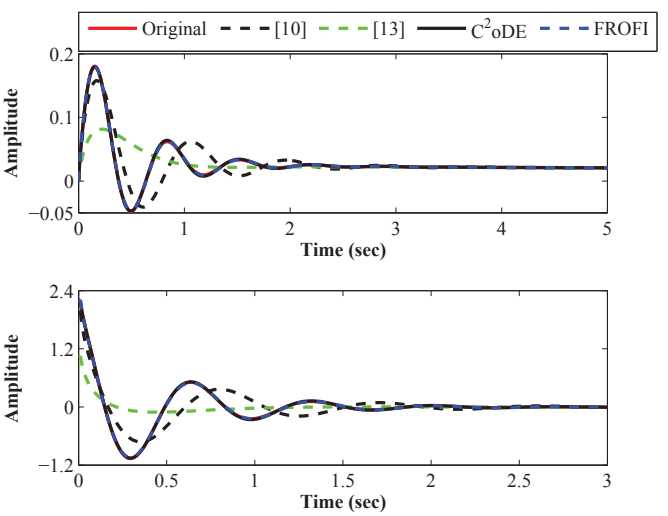

Fig. 7 Comparisons of step (top) and impulse (bottom) responses of the proposed ROMs with the literature for Example 2

posed approximants. Comparisons for the AME, APE, and MSE metrics are presented in Table 3. Results highlight that the suggested method significantly outperforms the ROMs designed using the Arnoldi and Lanczos algorithms. The $\|H\|_\infty$ achieved by the ROMs designed using C^2oDE (0.01836) and FROFI (0.01890) is also much smaller as compared to that of the models

reported in [13] (0.5365) and [10] (0.4514). The C^{2}oDE-based model attains marginally better accuracy than the FROFI-based design for the mean AME, max APE, mean APE, MSE for phase, and $\|H\|_\infty$ metrics.

The proposed ROMs distinctly outperform the cited literature about the step and impulse responses, as illustrated in Fig. 7. The time-domain responses of both the proposed compressed models nearly superimpose with the characteristics of the original system. The time-domain performance indices are compared with the published literature in Table 4 which shows that the proposed approach based on FROFI algorithm achieves the least values for all four error metrics.

Reference	IAE	ISE	ITAE	ITSE
[10]	0.07550	0.003275	0.1594	0.006061
[13]	0.06571	0.004808	0.1023	0.006629
C^{2}oDE	0.01960	0.000187	0.0455	0.000366
FROFI	0.01799	0.000159	0.0425	0.000307

Table 4 Comparisons with the literature about various time-domain performance indices for Example 2

3.3 Example 3

The higher-order commensurate system for this example is considered as

$$H_O(s) = \frac{s^{2.1} + 6.82s^{1.4} + 17.205s^{0.7} + 16.0012}{s^{2.8} + 4.79s^{2.1} + 9.58s^{1.4} + 9.21s^{0.7} + 3.69}. \tag{3.11}$$

The transfer function of the ROM obtained using the extended CFE method, as reported in [27], is given by

$$H_R(s) = \frac{0.71s^{0.7} + 5.4738}{s^{1.4} + 1.94s^{0.7} + 1.282}. \tag{3.12}$$

In order to compare with the reported model, the proposed ROM in the F-domain can be designed by selecting m and n as 1 and 2, respectively. The Lb and Ub values for all the coefficients (design variables) are chosen as 0 and 30, respectively. The optimal value of X based on the C^{2}oDE algorithm is determined as [5.0059 19.9948 5.0646 7.5679 4.6220]. The F-domain poles of the corresponding ROM are located at $-0.7471 \pm 0.5953\mathrm{i}$ $(= 0.9553\angle \pm 141.45^\circ)$, as presented in Fig. 8. The designed approximant satisfies the condition of F-plane stability since $|\theta_F| = 141.45^\circ$ exceeds $\theta_{Cr} = 63^\circ$. The C^{2}oDE-based model obtained after re-conversion from F-domain to s-domain is given below.

$$H_R(s) = \frac{5.0059s^{0.7} + 19.9948}{5.0646s^{1.4} + 7.5679s^{0.7} + 4.6220}. \tag{3.13}$$

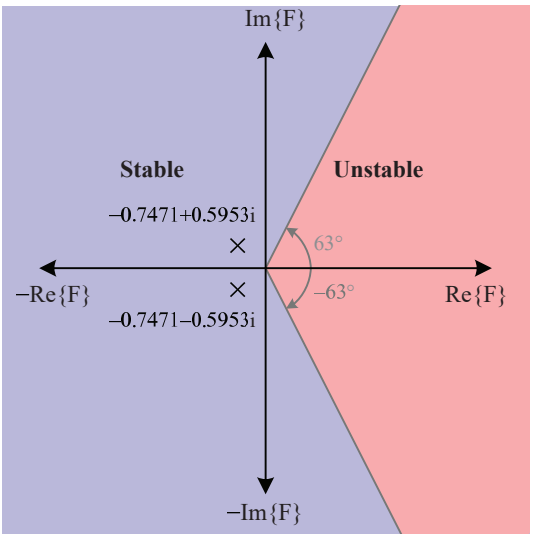

Fig. 8 Locations of poles in the F-plane for the proposed C^{2}oDE-based ROM in Example 3

The FROFI-based optimization routine yielded $X = [7.3765\ 29.8520\ 7.4625\ 11.3024\ 6.8968]$. The poles of $H_R(F)$ are located at $-0.7573\pm0.5922\mathrm{i}$ ($= 0.9614\ \angle\pm141.97°$). Since the critical phase $\theta_{Cr}(= 63°)$ is smaller than $|\theta_F|$ ($= 141.97°$), the reduced-order approximant attains the F-plane stability. The s-domain transfer function of the FROFI-optimized ROM is given as

$$H_R(s) = \frac{7.3765s^{0.7} + 29.8520}{7.4625s^{1.4} + 11.3024s^{0.7} + 6.8968}. \tag{3.14}$$

The magnitude and phase responses of the optimal ROMs are compared with the extended CFE-based model [27] in Fig. 9. Both the proposed designs attain better agreement with the responses of the large-scale model when compared to the cited literature. The various frequency response performance measures for the proposed and reported ROMs are compared in Table 5. These results confirm that the proposed approach achieves better accuracy when compared to the design published in [27]. For instance, the C^{2}oDE and FROFI-optimized ROMs achieve 0.02873 and 0.02761, respectively, for the $\|H\|_\infty$ metric; the same for the extended CFE-based model yields a much larger value (0.06233). The values of the error metrics for the ROM designed using C^{2}oDE and FROFI are nearly the same. Comparisons with [27] about $e(j\omega)$ and the absolute error in the step and impulse responses, as presented in Fig. 10, validate the better performance of the proposed designs. The proposed approximants distinctly outperform the reported literature [27] about the different time-domain performance metrics, as shown in Table 6. Comparisons also reveal that FROFI (0.4644) attains only marginal improvement over C^{2}oDE (0.4823) for the ITAE metric.

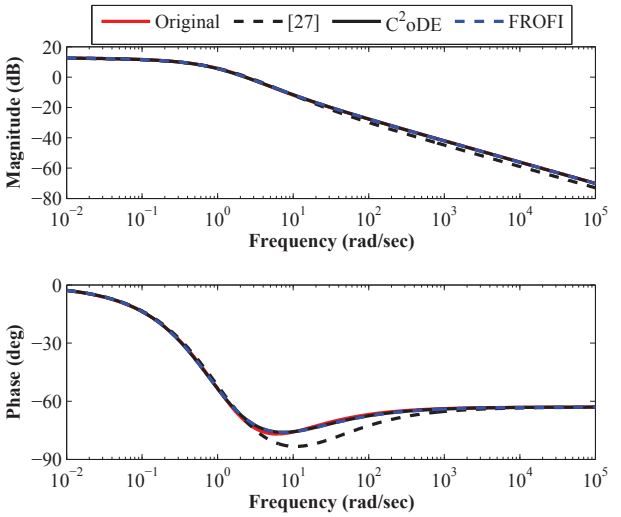

Fig. 9 Comparisons of magnitude and phase responses of the proposed ROMs with the literature for Example 3

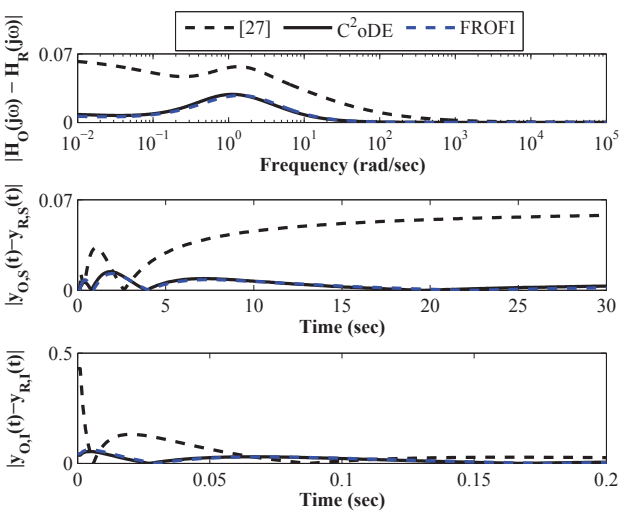

Fig. 10 Comparison of the proposed ROMs with the literature about the absolute error in frequency response (top), step response (middle), and impulse response (bottom) for Example 3

Error metric	[27]	C^2oDE	FROFI
Max AME	0.0621	0.0287	0.0268
Mean AME	0.0189	0.0044	0.0042
Max APE (rad)	0.1580	0.0276	0.0288
Mean APE (rad)	0.0388	0.0061	0.0063
MSE for magnitude	7.91×10^{-4}	6.28×10^{-5}	5.66×10^{-5}
MSE for phase (rad^2)	0.0039	8.38×10^{-5}	9.34×10^{-5}
$\|H\|_\infty$	0.06233	0.02873	0.02761

Table 5 Comparisons with the literature about various frequency-domain performance indices for Example 3

Reference	IAE	ISE	ITAE	ITSE
[27]	0.4249	0.02722	2.1690	0.11530
C^2oDE	0.1463	0.00510	0.4823	0.01242
FROFI	0.1474	0.00557	0.4644	0.01322

Table 6 Comparisons with the literature about various time-domain performance indices for Example 3

4 Conclusions

The F-plane angle condition is incorporated as a design constraint to attain stable ROMs for the fractional-order SISO systems in the presented approach. The proposed method is well-suited for diminution of commensurate FO systems since the s-plane model readily converts into an integer-order form in the F-domain. Optimal reduction of the large-scale system is carried out using C^2oDE and FROFI, with both the algorithms demonstrating similar performances. The superior accuracy of the proposed ROMs as compared to the recent literature is validated using various time- and frequency-domain performance measures. The $\{\|H\|_\infty$, ISE$\}$ achieved for the three design examples by the C^2oDE-based ROMs are $\{0.00421, 5.46\times10^{-6}\}$, $\{0.01836, 0.000187\}$, and $\{0.02873, 0.00510\}$, respectively; the same for the FROFI-based routine are $\{0.00440, 4.51\times10^{-6}\}$, $\{0.01890, 0.000159\}$, and $\{0.02761, 0.00557\}$, respectively. The achieved results are considerably lower than $\{0.04970, 8.05\times10^{-5}\}$, $\{0.45140, 0.003275\}$, and $\{0.06233, 0.02722\}$ yielded by the state-of-the-art.

Acknowledgements This article is based upon work from COST Action CA15225, a network supported by COST (European Cooperation in Science and Technology). The research results described in this paper are supported by the Czech Science Foundation, Project No. 19-24585S.

The authors would like to thank the reviewers for their valuable comments to improve the quality of this paper.

Conflict of interest

The authors declare that they have no conflict of interest.

References

1. Alagoz, B.B.: Hurwitz stability analysis of fractional order LTI systems according to principal characteristic equations. ISA Trans. **70**, 7–15 (2017). DOI: 10.1016/j.isatra.2017.06.005.
2. Bai, Z.J., Slone, R.D., Smith, W.T.: Error bound for reduced system model by Pade approximation via the Lanczos process. IEEE Trans.

Comput. Aided Des. Integr. Circuits Syst. **18**(2), 133–141 (1999). DOI: 10.1109/43.743719.

3. Benner, P., Ohlberger, M., Cohen, A., Willcox, K.: Model Reduction and Approximation: Theory and Algorithms. Society for Industrial and Applied Mathematics, Philadelphia (2017).
4. Biradar, S., Hote, Y.V., Saxena, S.: Reduced-order modeling of linear time invariant systems using big bang big crunch optimization and time moment matching method. Appl. Math. Model. **40**, 7225–7244 (2016). DOI: 10.1016/j.apm.2016.03.006.
5. Caponetto, R., Dongola, G., Fortuna, L., Petras, I.: Fractional Order Systems Modeling and Control Applications. World Scientific, New Jersey, USA (2010). DOI: 10.1142/7709.
6. Caponetto, R., Machado, J.T., Murgano, E., Xibilia, M.G.: Model order reduction: A comparison between integer and non-integer order systems approaches. Entropy **21**(9), 876 (2021). DOI: 10.3390/e21090876.
7. Das, S., Saha, S., Das, S., Gupta, A.: On the selection of tuning methodology of FOPID controllers for the control of higher order processes. ISA Trans. **50**, 376–388 (2011). DOI: 10.1016/j.isatra.2011.02.003.
8. Dastjerdi, A.A., Vinagre, B.M., Chen, Y.Q., HosseinNia, S.H.: Linear fractional order controllers: A survey in the frequency domain. Annu. Rev. Control. **47**, 51–70 (2019). DOI: 10.1016/j.arcontrol.2019.03.008.
9. Gao, Z.: Reduced order modelling method for linear fractional-order systems based on unsymmetric Lanczos algorithm. Contr. Decision. **31**(8), 1499–1504 (2016). DOI: 10.13195/j.kzyjc.2015.1006.
10. Gao, Z.: Stable model order reduction for fractional-order systems based on unsymmetric Lanczos algorithm. IEEE/CAA J. Automatica Sinica. **6**(2), 485–492 (2019). DOI: 10.1109/JAS.2019.1911399.
11. Garrappa, R., Maione, G.: Model order reduction on Krylov subspaces for fractional linear systems. IFAC Proc. **46**, 143–148 (2013). DOI: 10.3182/20130204-3-FR-4032.00138.
12. Jain, S., Hote, Y.V., Saxena, S.: Model order reduction of commensurate fractional-order systems using big bang–big crunch algorithm. IETE Tech. Rev. **37**(5), 453–464 (2020). DOI: 10.1080/02564602.2019.1653232.
13. Jiang, Y.L., Xiao, Z.H.: Arnoldi-based model reduction for fractional order linear systems. Int. J. Syst. Sci. **46**(8), 1411–1420 (2015). DOI: 10.1080/00207721.2013.822605.
14. Junior, F.A.C.A., Bessa, I., Pereira, V.M.B., Farias, N.J.S., de Menezes, A.R., de Medeiros, R.L.P., Filho, J.E.C., Lenzi, M.K., Júnior, C.T.C.: Fractional order pole placement for a buck converter based on commensurable transfer function. ISA Trans. **107**, 370–384 (2020). DOI: 10.1016/j.isatra.2020.07.034.
15. Kartci, A., Agambayev, A., Farhat, M., Herencsar, N., Brancik, L., Bagci, H., Salama, K.N.: Synthesis and optimization of fractional-order elements using a genetic algorithm. IEEE Access. **7**, 80233–80246 (2019). DOI: 10.1109/ACCESS.2019.2923166.

16. Khanra, M., Pal, J., Biswas, K.: Reduced order approximation of MIMO fractional order systems. IEEE J. Emerg. Sel. Top. Circuits Syst. **3**(3), 451–458 (2013). DOI: 10.1109/JETCAS.2013.2265811.
17. Krishna, B.T.: Recent developments on the realization of fractance device. Fract. Calc. Appl. Anal. **24**(6), 1831–1852 (2021). DOI: 10.1515/fca-2021-0079.
18. Lee, H.J., Chu, C.C., Feng, W.S.: An adaptive-order rational Arnoldi method for model-order reductions of linear time-invariant systems. Linear Algebra Appl. **415**(2–3), 235–261 (2006). DOI: 10.1016/j.laa.2004.10.011.
19. Liu, Y., Anderson, B.D.O.: Singular perturbation approximation of balanced systems. Int. J. Control. **50**, 1379–1405 (1989). DOI: 10.1080/00207178908953437.
20. Machado, J.A.T., Kiryakova, V: The chronicles of fractional calculus. Fract. Calc. Appl. Anal. **20**(2), 307–336 (2017). DOI: 10.1515/fca-2017-0017.
21. Mahata, S., Herencsar, N., Alagoz, B.B., Yeroglu, C.: A robust frequency-domain-based order reduction scheme for linear time-invariant systems. IEEE Access. **9**, 165773–165785 (2021). DOI: 10.1109/ACCESS.2021.3135279.
22. Mahata, S., Herencsar, N., Kubanek, D., Kar, R., Mandal, D., Goknar, I.C.: A fractional-order transitional Butterworth-Butterworth filter and its experimental validation. IEEE Access. **9**, 129521–129827 (2021). DOI: 10.1109/ACCESS.2021.3114182.
23. Mahata, S., Kar, R., Mandal, D.: Direct digital fractional-order Butterworth filter design using constrained optimization. Int. J. Electron. Commun. (AEU). **128**, 1–26 (2021). DOI: 10.1016/j.aeue.2020.153511.
24. Mahata, S., Kar, R., Mandal, D.: Optimal analog-to-digital transformation of fractional-order Butterworth filter using binomial series expansion with Al-Alaoui operator. Int. J. Circuit Theor. Appl. **49**(1), 44–79 (2021). DOI: 10.1002/cta.2908.
25. Mezura-Montes, E., Coello Coello, C.A.: Constraint-handling in nature-inspired numerical optimization: Past, present and future. Swarm Evol. Comput. **1**, 173–194 (2011). DOI: 10.1016/j.swevo.2011.10.001.
26. Moore, B.: Principal component analysis in linear systems: Controllability, observability, and model reduction. IEEE Trans. Autom. Control. **AC-26**, 17–32 (1981). DOI: 10.1109/TAC.1981.1102568.
27. Norouzzadeh, P.: Model order reduction of linear time-invariant commensurate fractional systems based on extended continued fraction method. In: Proc. 2020 Iran. Conf. Electr. Engg., 1–6, Tabriz, Iran (2020). DOI: 10.1109/ICEE50131.2020.9260728.
28. Podlubny, I.: Fractional Differential Equations. Academic Press, New York (1999).
29. Radwan, A.G., Soliman, A.M., Elwakil, A.S., Sedeek, A.: On the stability of linear systems with fractional-order elements. Chaos Solitons Fractals. **40**, 2317–2328 (2009). DOI: 10.1016/j.chaos.2007.10.033.

30. Saxena, S., Hote, Y.V., Arya, P.P.: Reduced-order modeling of commensurate fractional-order systems. In: Proc. 2016 14th Int. Conf. Control Automat. Robotics Vision, 1–6, Phuket, Thailand (2016). DOI: 10.1109/ICARCV.2016.7838855.
31. Shen, J., Lam, J.: H_∞ model reduction for positive fractional order systems. Asian J. Control. **16**(2), 441–450 (2014). DOI: 10.1002/asjc.694.
32. Tavakoli-Kakhki, M., Haeri, M.: Fractional order model reduction approach based on retention of the dominant dynamics: Application in IMC based tuning of FOPI and FOPID controllers. ISA Trans. **50**(3), 432–442 (2011). DOI: 10.1016/j.isatra.2011.02.002.
33. Tavakoli-Kakhki, M., Haeri, M.: Model reduction in commensurate fractional-order linear systems. Proc. Inst. Mech. Engineers I: J. Syst. Control Engg. **223**, 493–505 (2009). DOI: 10.1243/09596518JSCE690.
34. Tepljakov, A., Alagoz, B.B., Yeroglu, C., Gonzalez, E.A., Hosseinnia, S.H., Petlenkov, E., Ates, A., Cech, M.: Towards industrialization of FOPID controllers: A survey on milestones of fractional-order control and pathways for future developments. IEEE Access. **9**, 21016–21042 (2021). DOI: 10.1109/ACCESS.2021.3055117.
35. Tepljakov, A., Petlenkov, E., Belikov, J.: FOMCON: A MATLAB toolbox for fractional-order system identification and control. Int. J. Microelectron. Computer Sci. **2**(2), 51–62 (2011).
36. Tufenkci, S., Senol, B., Alagoz, B.B., Matusu, R.: Disturbance rejection FOPID controller design in v-domain. J. Adv. Res. **25**, 171–180 (2020). DOI: 10.1016/j.jare.2020.03.008.
37. Tufenkci, S., Senol, B., Matusu, R., Alagoz, B.B.: Optimal V-plane robust stabilization method for interval uncertain fractional order PID control systems. Fractal Fract. **5**(1), 3 (2021). DOI: 10.3390/fractalfract5010003.
38. Wang, B.C., Li, H.X., Li, J.P., Wang, Y.: Composite differential evolution for constrained evolutionary optimization. IEEE Trans. Syst. Man Cybern. Syst. **49**(7), 1482–1495 (2019). DOI: 10.1109/TSMC.2018.2807785.
39. Wang Y., Wang, B.C., Li, H.X., Yen, G.G.: Incorporating objective function information into the feasibility rule for constrained evolutionary optimization. IEEE Trans. Cybern. **46**(12), 2938–2952 (2016). DOI: 10.1109/TCYB.2015.2493239.
40. Xue, D., Chen, Y.Q.: Sub-optimal H_2 rational approximations to fractional order linear systems. In: ASME 2005 Int. Design Engg. Tech. Conf. Comput. Inform. Engg. Conf., 1527–1536, Long Beach, California (2005).
41. Yang, Q., Chen, D., Zhao, T., Chen, Y.Q.: Fractional calculus in image processing: a review. Fract. Calc. Appl. Anal. **19**(5), 1222–1249 (2016). DOI: 10.1515/fca-2016-0063.